STABILITY OF THE DRIVE BEAM IN THE DECELERATOR OF CLIC

D. Schulte, CERN, Geneva

Abstract

The RF power necessary to accelerate the main beam in the compact linear collider (CLIC) is generated by decelerating high-intensity low energy drive beams in 44 decelerators. Recently new decelerating structures (PETS, power extraction and transfer structures) have been developed. In these structures the RF energy travels with particularly high group velocity, which can affect efficiency and transverse stability. The paper considers the transverse beam stability in the decelerator as well as the longitudinal effects in the presence of dynamic and static imperfections.

1 INTRODUCTION

In CLIC [1] a sequence of 22 drive beam decelerators run along each of the two main linacs. In these decelerators a high-intensity low-energy drive beam is decelerated in power extraction and transfer structures (PETS); for the structure parameters [2] see Table 1. Each of them feeds two main linac structures with the power that it extracts from the drive beam. During the deceleration a large energy spread develops in the drive beam, which initially is almost mono-energetic. While some particles lose hardly any energy, many are strongly decelerated, some down to 10% of their intial energy. The decelerator optics is based on a simple FODO lattice with a quadrupole spacing of $1.115\,\mathrm{m}$. Before each quadrupole a beam position monitor (BPM) is placed and between each pair of quadrupoles a PETS. The phase advance per cell is 88° and the strength of the magnets is scaled to keep the phase advance and beta-functions constant for the lowest energy particles. This ensures that the whole beam is contained within the envelope of these low energy particles [3].

The parameters of the drive beam are listed in Table 2. The bunch spacing is $\Delta z = 2\,\mathrm{cm}$. During the first $25\,\mathrm{ns}$, larger gaps exist between some bunches (always multiples of $2\,\mathrm{cm}$). This modulates the pulse intensitiy in order to compensate for the beam loading in the main linac [4].

2 STRUCTURE DETUNING

In previous studies [5], the fundamental frequency of the PETS structure was chosen to be the same as the RF one wanted to generate, and the bunch repetition frequency was a subharmonic of the other two. In these structures, the deceleration of the bunches was dominated by the long-range longitudinal wakefield. With these chosen parameters the efficiency of converting the drive beam power into RF power was maximised. The particle that is decelerated most determines the maximum deceleration. Therefore the efficiency η of transforming drive-beam power into RF power is determined by the ratio of average deceleration of the particles to the maximum deceleration ΔE in a structure. As a function of the output power P and the beam current I, we find $\eta \propto P/(\Delta E)I$.

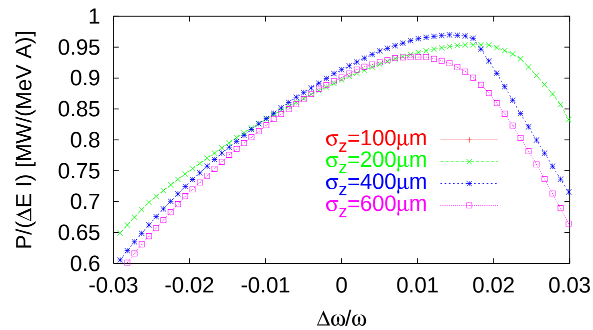

Figure 1: The output power of the PETS as a function of the frequency detunig.

In the present structure the single bunch longitudinal wakefield plays an important role. It decelerates the tail of the bunch, which is thinly populated, more than the highly populated centre. Thus the efficiency is reduced. It can be increased again by using PETS with a frequency that is slightly higher than the required RF (about 1.5%). The

Table 1: Parameters of the PETS.

Parameter	symbol	value
fundamental frequency	f_{RF}	$30.45\,\mathrm{GHz}$
impedance (linac)	R'/Q	$2 \times 122\,\Omega/\mathrm{m}$
group velocity of fund. mode	$\beta_\parallel$	0.85
frequency of dipole mode	$f_\perp$	$30.75\,\mathrm{GHz}$
amplitude of transv. wake	$W_\perp$	$1480\,\mathrm{V/pCm^2}$
group velocity of dipole mode	$\beta_\parallel$	0.88
damping of dipole mode	Q	≤ 50
active length	L_c	$0.8\,\mathrm{m}$
iris radius	a	$12.5\,\mathrm{mm}$

Table 2: Some drive beam parameters.

Parameter	symbol	value
Initial beam energy	E_0	$2.0\,\mathrm{GeV}$
initial bunch length	σ_z	$400\,\mu\mathrm{m}$
particles per bunch	N	6.1×10^{10}
transverse emittances	ϵ_x,ϵ_y	$100\,\mu\mathrm{m}$

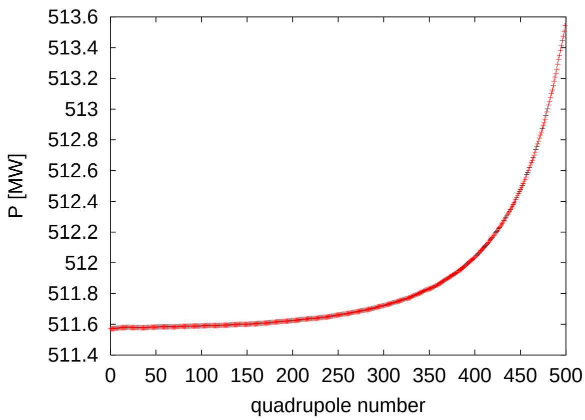

Figure 2: The power production along the linac.

frequency of the bunches is not modified. In this case the multi-bunch wakefields decelerate the front of the bunches more than the tail, counter-balancing the effect of the single bunch wakefield. The efficiency increases, as can be seen in Fig. 1.

3 LONGITUDINAL BEAM STABILITY

The drive beam produces the RF power for the main beam. A variation of the timing of the drive beam therefore changes the phase of the main linac RF. This can lead to energy errors of the main beam and to a growth of its transverse emittance. The tolerance of the RF phase error has been studied [6]. For a coherent phase error along the whole linac, the amplitude of the phase error must be limited to less than $0.2°$.

Two main effects contribute to the longitudinal motion of the particles within the bunch; they travel with less than the speed of light and, because of the betatron motion, they have small angles with respect to the reference trajectory. Compared to the main beam that moves closer to the speed of light and with smaller angles, the phase of the drive will vary along the decelerator. As long as the variation is static it has no effect on the main beam, since the relative phase of PETS and main linac structures can be tuned. However the longitudinal shape of the bunches will change slightly along the decelerator, leading to a slightly changing power production. The beam dynamics simulation code PLACET [7] has been modified to include the longitudinal motion of particles within the bunch. The simulation shows that the variation of the RF power along the decelerator is quite small, see Fig. 2. Since it is also static it should not lead to any problem.

A transverse jitter of the beam increases the betatron motion of all particles leading to an uncorrectable longitudinal jitter of the drive beam. Towards the end of the decelerator, the phase error grows more rapidly since the beam size and thus the oscillation amplitude is increasing. In Fig. 3 the local phase errors for initial offsets of $\Delta y = \sigma_y$ and $\Delta y = 2\sigma_y$ are shown. The error is proportional to $\Delta\phi \propto (\Delta y)^2$.

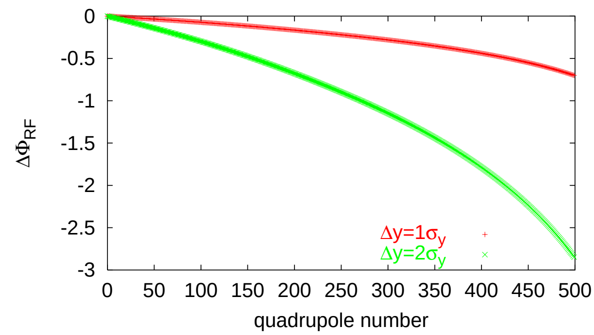

Figure 3: Logitudinal phase error of the drive beam for an initial offset.

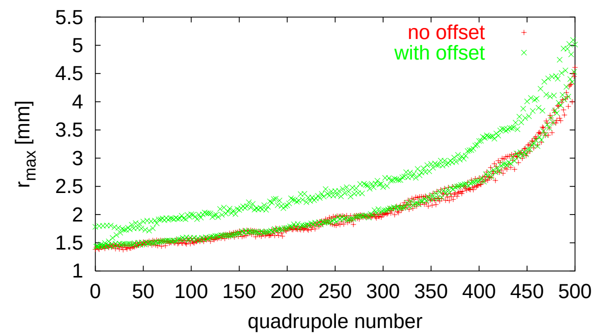

Figure 4: The 4σ-envelope of the beam in the decelerator for an on-axis beam and one with an initial offset $\Delta y = \sigma_y$.

For $\Delta y = \sigma_y$ the average phase error along the decelerator is $\Delta\phi \approx 0.25°$. The effect of a horizontal jitter is comparable, and also that of an angle jitter of $\Delta x' = \sigma_{x'}$ or $\Delta y' = \sigma_{y'}$. Therefore, the tolerance for the intitial jitter is about $(\Delta x/\sigma_x)^2 + (\Delta y/\sigma_y)^2 + (\Delta x'/\sigma_{x'})^2 + (\Delta y'/\sigma_{y'})^2 \leq 0.9^2$.

Transverse beam jitter leads not only to a variation of the drive-beam phase; the amplitude of the produced RF is also affected. The energy spread in each bunch is quite large and consequently the amplitude of the betatron motion for these particles is different. This leads to a longitudinal deformation of the bunch in addition to the one for an on-axis beam. For an offset of $\Delta y = \sigma_y$, the average power production along the linac is increased by 0.017%. This effect is therefore quite small compared to the phase error.

Transverse jitter in the beamline that transports the drive beam to the decelerator remains to be studied. It is planned to reduce its effect by using feedbacks at the entrance of the drive beam decelerator where the beam has to go through an arc. This should also allow to minimise the impact of incoming transverse beam jitter within the decelerator.

4 TRANSVERSE BEAM STABILITY

Figure 4 shows the envelope of two 4σ beams. In the first case the beam was on-axis. The envelope increases slowly along the machine, since the motion of the particles is adiabatically undamped because of the decrease in energy. The

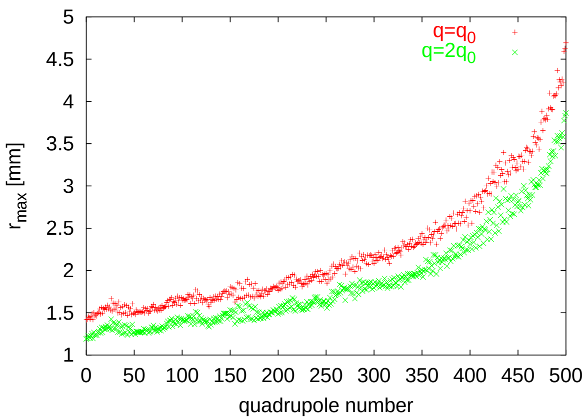

Figure 5: The 3σ-envelope of the drive beam after beam-based correction of the static imperfections. The maximum for 100 simulated machines is shown.

other beam was offset by $\Delta y = \sigma_y$ at the entrance of the decelerator. Its size alternates because of the different vertical spot size in focusing and defocusing quadrupoles. The envelope does not grow significantly faster than the one of the on-axis beam. The limit for the transverse jitter derived from the transverse effects seems to be less stringent than the derived from the longitudinal motion discussed before.

5 BEAM-BASED CORRECTION

The drive beam decelerators will be aligned with the same sophisticated system of wires and lasers that is used for the main linac [8]. However, for the simulation, more pessimistic alignment errors are assumed. The pre-alignment of the girders has been simulated for 100 cases [9]. The wires define a sequence of straight lines. One tries to align the individual elements to these reference lines. It is assumed that the error of the element position with respect to the reference line follows a Gaussian distribution with an RMS of $100\,\mu\mathrm{m}$ for all elements. The BPM resolution is assumed to have an RMS of $10\,\mu\mathrm{m}$. The alignment is performed in two main steps. First a low-intensity low-emittance beam is used to align the BPMs using the ballistic method [10]. In this procedure the decelerator is divided into bins, each containing a small number of quadrupoles (typically 12). Then one bin after the other is corrected. The quadrupoles in the bin are switched off and the beam is centred in the last BPM of the bin. The other BPMs are then aligned to the beam; this step can be done by mechanically moving the BPMs or by electronically adding offsets. The quadrupoles in the bin are switched on again and moved transversely to maintain the beam position in the BPMs. Once this correction step is finished the real drive beam is injected into the decelerator, first at low intensity which is then slowly increased to its nominal level. During this step, a permanent correction of the quadrupoles is performed to keep the beam position in the BPMs constant. The resulting maximum 3σ-envelope for 100 machines is well confined, see Fig. 5.

6 SCALING WITH OUTPUT POWER

Due to changes of the design for the main linac structure the required output power of the PETS may differ from the present value. Therefore the dependence of the beam stability on the power requirement is discussed. Here the assumption is made that neither the structure geometry nor the lattice is changed and that the ratio of initial to final beam energy is maintained. In this case the beam current scales as $I \propto \sqrt{P}$ and consequently the initial beam energy as $E_0 \propto \sqrt{P}$. The angle kick induced in the beam by a structure with an offset is proportional to I/E, where the energy E that the beam has at the given point is, with the given scaling, proportional to E_0. The angle is therefore independent of the beam intensity. The same is true for the quadrupoles. At higher power, the beam envelope will thus not be larger than at lower power. Due to the smaller initial beam size (smaller real emittance) it will be even somewhat smaller. Simulations of the static alignment confirm these predictions, see Fig. 5.

An initial beam jitter can be treated in a similar fashion. Independent of the beam current, the same absolute beam jitter will lead to the same beam size growth and phase error. For the same relative jitter, the effects will thus be smaller at higher currents.

7 CONCLUSION

The drive beam decelerator has been studied using new PETSs. Their longitudinal and transverse modes have a high group velocity; detuning of the fundamental mode is therefore advantageous to maintain a high efficiency. In the presence of incoming transverse beam jitter, the transverse beam stablity is good. However, to achieve a good phase stability of the produced RF, the transverse jitter needs to be limited. Beam-based correction of static imperfections of the beam line elements can be successfully applied.

8 REFERENCES

[1] G.Guignard (ed.). CERN-2000-8.

[2] I. Syratchev and W. Bruns. CERN/PS 2001-046 (RF) and Proc. PAC 2001, Chicago, Illinois, USA.

[3] A. Riche. CLIC-Note 266 (1994).

[4] D. Schulte and I. Syratchev. CLIC-Note 453 and Proc. Linac 2000, Monterey, CA, USA.

[5] A. Riche and D. Schulte. CLIC-Note 380 and Proc. LINAC 1998, Chicago, Illinois, USA.

[6] D. Schulte. CLIC-Note 432.

[7] D. Schulte. CLIC-Note 437 and and Proc. EPAC 2000, Vienna, Austria.

[8] W. Coosemans. Private communication.

[9] F. Becker. Private communication.

[10] T. Raubenheimer and D. Schulte. CLIC-Note 495 and Proc. PAC 1999, New York, USA.